Biointerface Research in Applied Chemistry
Platinum Open Access Journal (ISSN: 2069-5837)

Article
Volume 12, Issue 6, 2022, 7994 - 8002
https://doi.org/10.33263/BRIAC126.79948002

A Facile Synthesis of Fe_3O_4@SiO_2@ZnO for Curcumin Delivery

Somayeh Sadighian [1,2,*], Kimia Sharifan [1], Akram Khanmohammadi [1], Matine Kamkar Rohani [1]

[1] Department of Pharmaceutical Biomaterials, School of Pharmacy, Zanjan University of Medical Sciences, Zanjan, Iran
[2] Zanjan Pharmaceutical Nanotechnology Research Center, School of Pharmacy, Zanjan University of Medical Sciences, Zanjan, Iran
* Correspondence: somayeh.sadighian@gmail.com;

Scopus Author ID 26325122200
Received: 2.10.2021; Revised: 5.11.2021; Accepted: 8.11.2021; Published: 5.12.2021

Abstract: This paper proposed an engineered silica-coated Fe_3O_4 with ZnO nanoparticle, prepared by a coprecipitation/Stöber method as a curcumin delivery system. To this end, the structural characterization of the nanocomposite was performed by Fourier transform infrared spectroscopy (FT-IR), ray diffraction (XRD), VSM, and TEM. The findings show that the synthesized nanocomposite has a semispherical structure with an average particle size of 50-70 nm and excellent magnetization properties (21.4 emu/g).

Keywords: magnetite; zinc nanoparticles; silica; curcumin.

1. Introduction

In recent decades, magnetic nanoparticles have received much attention in medical applications due to their magnetic properties, easy surface modification, and high biocompatibility [1-4]. Magnetite is widely used in drug delivery [5,6], magnetic imaging [6-8], and catalytic studies. One of the applications of these nanoparticles is their use in targeted drug delivery. The core-shell structure of magnetic nanoparticles is highly regarded as a targeted and controlled drug delivery system [9]. With controlled drug delivery, nanocarriers can overcome the problems of conventional drugs, such as low solubility and rapid clearance of the drug from the body [10]. Targeted drug delivery leads to the drug delivery to the target tissue and will have the least side effects on other tissues [11]. Magnetic nanoparticles such as Fe_3O_4 are highly regarded for their magnetic properties, low toxicity, and biocompatibility [12,13]. However, magnetite nanoparticles have high surface energy which causes them to be aggregate. These nanoparticles are also prone to oxidation in the air, which reduces their magnetic properties. Therefore, to prevent these problems, they must be functionalized by various polymers [14], silica [2,15,16], and metals [10]. Silicon is a biocompatible trace element in the human body and has been the subject of important research due to its distinctive structural properties such as large surface area and specific surface area [17]. Due to the network structure, the rate of biological degradation is slow, and therefore, it can accumulate in the body, limiting its biomedical applications [18]. Silica is stable in acidic conditions and has hydroxyl groups that bind magnetite to various biological ligands. Silica is non-toxic and used as a vitamin supplement and food additive [19]. In this study, we used the Stöber method

to synthesize silica [20]. Zinc oxide (ZnO) is very important in the treatment of cancer. Zinc oxide is present in various structures, including nanorods, nanospheres, and nanoparticles. It is non-toxic and has antibacterial properties. It is also biocompatible and serves as a potential candidate for drug delivery [21].

CUR [22] is a polyphenol substance whose anti-cancer properties have been proven. It is prepared in different forms of medicine and is used in different types of malignancy, anti-inflammatory, antioxidant, antimicrobial. Curcumin can be found in various molecules in the cell, such as proteins such as thioredoxin reductase, cyclooxygenase 2 (COX-2), protein target kinase C (PKC), 5-lipoxygenase (5-LO). Curcumin will have little effect due to poor water solubility and low bioavailability. One way to overcome this problem is to use nanoparticles.

In a recent study, Fe_3O_4 was synthesized, and then the silica-coated nanoparticles were fabricated, and finally, ZnO nanoparticles were added to the structure (scheme 1). We used nanoparticles prepared for drug delivery of curcumin (CUR). Considering the above issues, the main objective of this study was to prepare and characterize the nanocomposite of silica and iron oxide by coprecipitation method and evaluate its potential as a drug delivery system with a pH-sensitive property.

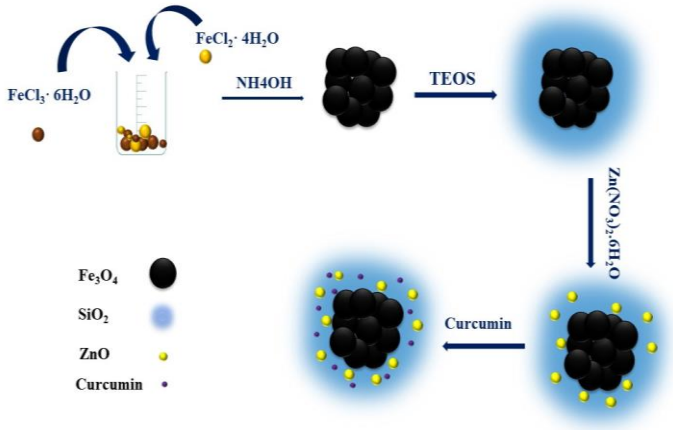

Scheme 1. Synthetic Procedure of nanocomposite.

2. Materials and Methods

2.1. Materials and reagents.

Iron (II) chloride tetra-hydrate ($FeCl_2.4H_2O$) and Iron (III) chloride hexahydrate ($FeCl_3.6H_2O$), Zinc nitrate hexahydrate ($ZnNO_3.6H_2O$), dimethyl-form-amide (DMF), Curcumin (CUR), sodium hydroxide (NaOH), and tetraorthosilicates (TEOS, $C_8H_{20}O_4Si$) purchased from Merck Company. Ammonia solution (NH_4OH, 25%) was obtained from Sigma-Aldrich.

2.2. Synthesis of Fe_3O_4 nanoparticle.

Fe_3O_4 magnetic nanoparticles synthesized via co-precipitation method [23,24]. Briefly, 2 mmol $FeCl_3.6\ H_2O$ and 1mmol $FeCl_2.4\ H_2O$ were mixed in 50 mL of distilled water and heated to 80 ºC under vigorous stirring and N_2 gas. Then 20 ml of NH_4OH was added drop by drop. The black precipitates (F) were separated by an external magnet and washed with distilled water three times, and finally dried in the oven at 60 ºC. The relevant chemical reaction can be described with follows equation (1):

$$Fe^{2+} + 2Fe^{3+} + 8OH^- \rightarrow Fe_3O_4 + 4H_2O \quad (1)$$

2.3. Synthesis of Fe_3O_4@SiO_2 nanocomposite.

Fe_3O_4-SiO_2 core-shell nanoparticle were synthesized by Stöber method [25]. Briefly, 0.1 g Fe_3O_4 and mixture solution containing 80 ml ethanol and 20 ml deionized water were dispersed in an ultrasonic bath for 1 h. Then, ammonium hydroxide (1 mL) and 0.3 ml TEOS were added dropwise. The mixture was mechanically stirred for 4 h. Finally, the Fe_3O_4-SiO_2 (FS) was separated by an external magnet, washed three times with distilled water, and dried in an oven at 60-70 ºC.

2.4. Synthesis of Fe_3O_4@SiO_2@ZnO mesoporous.

0.5 g of synthesized Fe_3O_4–SiO_2 powder was dispersed in 50 ml of DMF by ultrasonic bath, and 0.3 g of $ZnNO_3 \cdot 6H_2O$ was dissolved in 50 ml of DMF then added to the initial solution. The colloids were sonicated for another 30 min. 2 ml of NaOH (0.5 M) solution was added dropwise to the previous ingredients [26]. The colloids were sonicated for another 1 h and maintained at room temperature for 1 day [27]. Finally, the Fe_3O_4-SiO_2-ZnO (FSZ) nanocomposite was separated using an external magnet, washed with distilled water three times, and dried in an oven at 60 ºC.

2.5. Preparation of curcumin-loaded FSZ nanocomposite.

Briefly, 50 mg FSZ were dispersed in 5 mL ethanol under stirring at 500 rpm, and 10 mg CUR dissolved in 5 mL ethanol and then added to the suspension. The mixture was kept stirring for 20 hours under dark conditions at room temperature [28,29]. The CUR-loaded FSZ nanocomposite was collected by an external magnet then washed with distilled water and ethanol to remove unloaded CUR. CUR loaded FSZ nanocomposite dried in a vacuum oven at 30 ºC for 12 h. To determine the loading efficiency, 5.0 mg of Cur-FSZ were redispersed in 10 mL of ethanol. To specify the amount of unloaded curcumin, the centrifuged solution was collected and analyzed for drug content by UV–Vis spectrophotometry at a wavelength of 425 nm. Then the amount of DL and EE was calculated using the equation (2) and (3), respectively:

$$\% \text{ DL} = (\text{Weight of drug in nanocomposite})/(\text{weight of nanocomposite}) \quad (2)$$

$$\% \text{ EE} = (\text{total drug-free drug})/(\text{total drug}) \times 100 \quad (3)$$

2.6. Drug release study of CUR-FSZ nanocomposite.

CUR release behavior of the CUR-FSZ nanocomposite was studied in PBS solution with different pHs (pH 7.4 and 5.5) containing 0.5 % tween 80. Briefly, 5 mg CUR-FSZ nanocomposite was placed into a dialysis bag (Mw 12 kDa) and immersed in 20 ml of PBS solution, then incubated at 37 ºC in a shaker incubator (SI-1000, Heidolph, Germany) under 150 rpm. At a specified interval, 1.0 ml of solution was replaced with 1.0 mL of fresh buffer solution. The amount of drug released was determined using UV-visible spectroscopy at a wavelength of 425 nm. All the release studies were carried out in triplicate.

3. Results and Discussions

3.1. FT-IR analysis.

FT-IR spectra analysis was used to identify the synthesized structure, and the results are shown in Figure 1. The broad peak at 3425cm^{-1} and 1635 cm^{-1} are assigned to stretching

and bending vibrations of the hydroxyl group of water, respectively. The characteristic peak for the vibration mode of the Fe-O bond of Fe_3O_4 is located at 582 cm^{-1} (Figure 1 (a)). By comparing Figure 1 (a) and (b), can be seen new peak around 1091, 796, and 466 cm^{-1} in the FT-IR spectrum of FS, which is related to asymmetric stretching, symmetric stretching, and vibration modes of Si-O-Si bonds that demonstrate SiO_2 on the surface of Fe_3O_4 nanoparticles [4]. The peak of the Zn-O is at 462 cm^{-1} that due to overlapping with the peak at 466 cm^{-1} belongs to Si-O-Si, and Fe-O did not appear [30]. In the FT-IR spectrum of CUR-FSZ (Figure 1 (d)), CUR-FSZ Curcumin index peaks overlap with previous peaks, and the carbonyl group peak is seen at 1520 cm^{-1} [31].

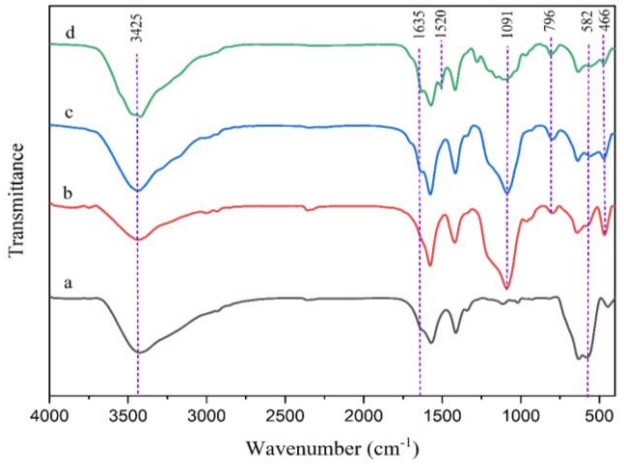

Figure 1. FT-IR spectra of **(a)** F**; (b)** FS; **(c)** FSZ; **(d)** CUR-FSZ.

3.2. X-ray diffraction analysis (XRD).

The crystallinity of the synthesized samples was investigated with X-ray diffraction analysis (XRD). Figure 2 shows the XRD patterns of synthesized nanoparticles. In Figure 2a, six characteristic peaks at 30.2, 35.6, 43.3, 53.8, 57.3, and 63 were corresponding to the (220), (311), (400), (422), (511), and (440) crystal planes of a pure Fe_3O_4, respectively (JCPDS No. 19-0629).

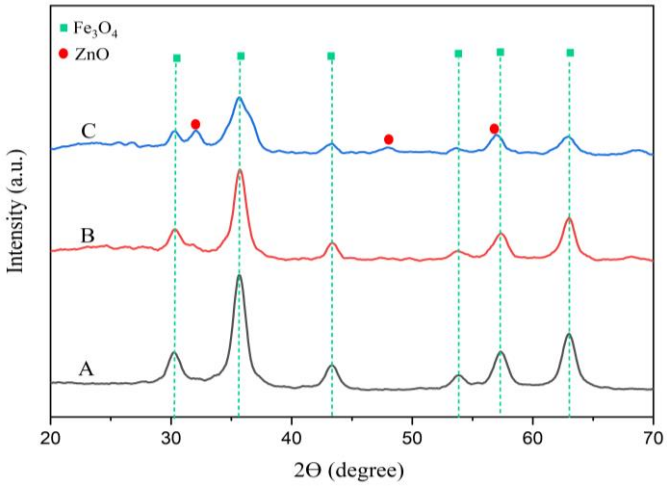

Figure 2. XRD patterns of **(a)** F; **(b)** FS; **(c)** FSZ.

The resulting pattern indicating that Fe_3O_4 have a spinal structure Figure 2b shows the XRD diffraction pattern of FS. Since silica compounds are amorphous, no peak is observed in this area. A slight decrease in the intensity of FS intensity diffraction peaks compared to F can cause the presence of amorphous silica. In Figure 2c, there are obvious diffraction peaks at

32.1, 47.9, and 56.9 corresponds to the crystal planes of (100), (102), and (110) of ZnO, respectively (JCPDS No. 36-1451), which confirm that ZnO particles have on the FSZ nanocomposite [32]. The XRD patterns indicate that the crystalline structure of the naked system (Fe_3O_4) has not changed during the different levels.

3.3. Magnetic properties.

A vibrating sample magnetometer (VSM) was used to investigate the magnetic properties of synthesized materials. As shown in Figure 3, magnetic hysteresis loops do not show obvious remanence or coercivity at room temperature, indicating that all samples have superparamagnetic properties. The magnetic saturation values (Ms) of F, FS, and FSZ were 56.7, 27.5, and 21.4 emu/g, respectively. They decrease in Ms value after coating confirms that it has been done successfully. Of course, the Ms value of FSZ was still high enough to be isolated using an external magnetic force [33,34].

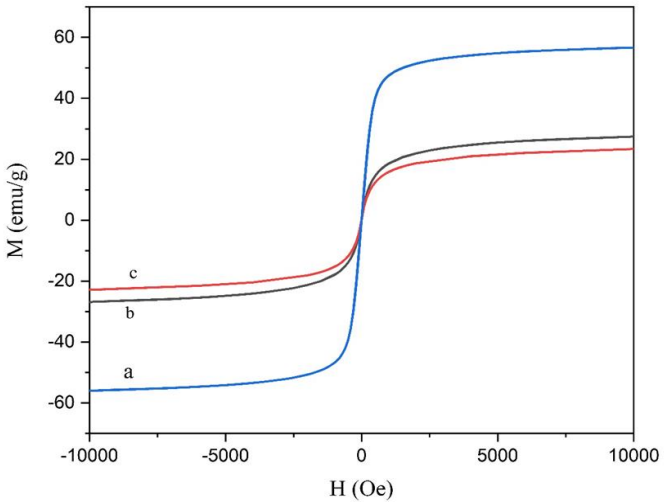

Figure 3. Magnetic hysteresis loops of the products at room temperature of (**a**) F; (**b**) FS; (**c**) FSZ.

3.4. Morphological structure analysis.

A transmission electron microscope (TEM) was applied to investigate the synthesized magnetic nanocomposite's morphological characteristics and size distribution.

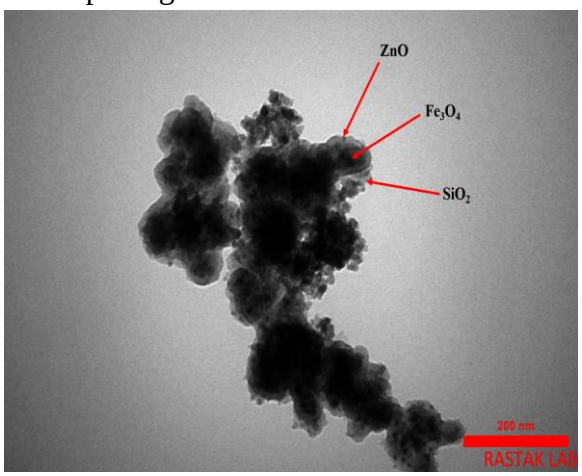

Figure 4. TEM image of FSZ nanocomposite.

In TEM images of FSZ (Figure 4), the presence of Fe_3O_4 nanoparticles at the core of the nanocomposite as dark points in the images is quite evident. The magnetic core appears to be somewhat aggregated and clustered, and the SiO_2 is covered around them. The particles

have an average diameter of 50-70 nm. Also, it can be seen that ZnO has been successfully deposited on the surface of FS nanoparticles.

3.5. Drug loading and release.

To investigate the capability of loading and release behaviors of FSZ nanocomposite as a nanocarrier, CUR was used as a model drug. DL and EE percentages were calculated at 20 % and 76 %, respectively. The release profile of CUR is shown in Figure 5 .In 12 h, Bare drug had burst released, almost 100%, whereas FSZ-CUR nanocomposite is shown sustained and controlled drug release behavior.

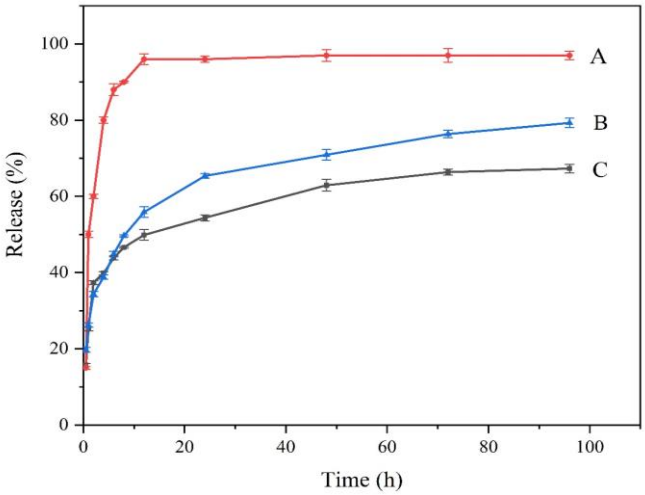

Figure 5. Release profiles of CUR (A in pH = 7.4) and FSZ-CUR (B in pH = 5.5, C in pH = 7.4). Each data point represents the mean ± S.D. (n = 3).

In FSZ-CUR nanocomposite, up to 45% and 55% CUR was released in physiological condition (pH 7.4) and acidic condition (pH 5.5), respectively. This coating layer has made a diffusion barrier for the drug released, leading to a sustained release behavior [35]. Also, the difference in release profiles in different pH was noticeable. It can be related to the cleavage of the chemical bond between magnetite and CUR in acidic conditions (Figure 5b compared with 5c).

4. Conclusions

In summary, we synthesized a magnetic nanocomposite based on silica-coated magnetic nanoparticles with zinc nanoparticles (FSZ). The designed nanocomposite is made with a suitable size and has desirable magnetic properties. The system designed to deliver curcumin in acidic and neutral environments was used. Release studies have shown that the amount of drugs released in acidic environments is slightly higher than in the natural environment.

Funding

This research received no external funding.

Acknowledgments

This work was supported by the Zanjan University of Medical Sciences (Grant No. A-12-928-22).

Conflicts of Interest

The authors declare no conflict of interest.

References

1. Karami, Z.; Sadighian, S.; Rostamizadeh, K.; Hosseini, S.H.; Rezaee, S.; Hamidi, M. Magnetic brain targeting of naproxen-loaded polymeric micelles: pharmacokinetics and biodistribution study. *Materials Science and Engineering* **2019**, *100*, 771-780, https://doi.org/10.1016/j.msec.2019.03.004.
2. Kermanian, M.; sadighian, s.; Ramazani, A.; Naghibi, M.; Hosseini, S.H. A Novel Mesoporous Superparamagnetic Hybrid Silica/Hydroxyapatite Nanocomposite as MRI Contrast Agent. ChemNanoMat **2021**, *7*, https://doi.org/10.1002/cnma.202000625.
3. Sadighian, S.; Abbasi, M.; Arjmandi, S.; Karami, H. Dye removal from water by zinc ferrite-graphene oxide nanocomposite. *Progress in Color, Colorants and Coatings* **2018**, *11*, 85-92.
4. Kermanian, M.; Sadighian, S.; Naghibi, M.; Khoshkam, M. PVP Surface-Protected Silica Coated Iron Oxide Nanoparticles for MR Imaging Application. *Journal of Biomaterials Science, Polymer Edition* **2021**, 1-11, https://doi.org/10.1080/09205063.2021.1916869.
5. Kermanian, M.; Naghibi, M.; Sadighian, S. One-pot hydrothermal synthesis of a magnetic hydroxyapatite nanocomposite for MR imaging and pH-Sensitive drug delivery applications. *Heliyon* **2020**, *6*, e04928, https://doi.org/10.1016/j.heliyon.2020.e04928.
6. Sadighian, S.; Bayat, N.; Najaflou, S.; Kermanian, M.; Hamidi, M. Preparation of Graphene Oxide/Fe3O4 Nanocomposite as a Potential Magnetic Nanocarrier and MRI Contrast Agent. *Chemistry Select* **2021**, *6*, 2862-2868, https://doi.org/10.1002/slct.202100195.
7. Kermanian, M.; Sadighian, S.; Ramazani, A.; Naghibi, M.; Khoshkam, M.; Ghezelbash, P. Inulin-Coated Iron Oxide Nanoparticles: A Theranostic Platform for Contrast-Enhanced MR Imaging of Acute Hepatic Failure. *ACS Biomaterials Science & Engineering* **2021**, https://doi.org/10.1021/acsbiomaterials.0c01792.
8. Tadic, M.; Kopanja, L.; Panjan, M.; Lazovic, J.; Tadic, B.V.; Stanojevic, B.; Motte, L. Rhombohedron and plate-like hematite (α-Fe2O3) nanoparticles: Synthesis, structure, morphology, magnetic properties and potential biomedical applications for MRI. *Materials Research Bulletin* **2021**, *133*, 111055, https://doi.org/10.1016/j.materresbull.2020.111055.
9. Zhao, Y.; Zhang, H.; Yang, X.; Huang, H.; Zhao, G.; Cong, T.; Zuo, X.; Yang, S.; Pan, L. In situ construction of hierarchical core–shell Fe3O4@ C nanoparticles–helical carbon nanocoil hybrid composites for highly efficient electromagnetic wave absorption. *Carbon* **2021**, *171*, 395-408, https://doi.org/10.1016/j.carbon.2020.09.036.
10. Qiu, H.; Cui, B.; Li, G.; Yang, J.; Peng, H.; Wang, Y.; Li, N.; Gao, R.; Chang, Z.; Wang, Y. Novel Fe3O4@ ZnO@ mSiO2 nanocarrier for targeted drug delivery and controllable release with microwave irradiation. *The Journal of Physical Chemistry C* **2014**, *118*, 14929-14, https://doi.org/10.1021/jp502820r.
11. Shen, L.; Li, B.; Qiao, Y. Fe3O4 nanoparticles in targeted drug/gene delivery systems. *Materials* **2018**, *11*, 324, http://doi.org/10.3390/ma11020324.
12. Singh, A.; Sahoo, S.K. Magnetic nanoparticles: a novel platform for cancer theranostics. *Drug Discovery Today* **2014**, *19*, 474-481, https://doi.org/10.1016/j.drudis.2013.10.005.
13. Wen, W.; Wu, L.; Chen, Y.; Qi, X.; Cao, J.; Zhang, X.; Ma, W.; Ge, Y.; Shen, S. Ultra-small Fe_3O_4 nanoparticles for nuclei targeting drug delivery and photothermal therapy. *Journal of Drug Delivery Science and Technology* **2020**, *58*, 101782, https://doi.org/10.1016/j.jddst.2020.101782.
14. Khalkhali, M.; Rostamizadeh, K.; Sadighian, S.; Khoeini, F.; Naghibi, M.; Hamidi, M. The impact of polymer coatings on magnetite nanoparticles performance as MRI contrast agents: a comparative study. *DARU Journal of Pharmaceutical Sciences* **2015**, *23*, 1-12, https://doi.org/10.1186/s40199-015-0124-7.
15. Ji, Y.; Song, S.; Li, X.; Lv, R.; Wu, L.; Wang, H.; Cao, M. Facile fabrication of nanocarriers with yolk-shell mesoporous silica nanoparticles for effective drug delivery. *Journal of Drug Delivery Science and Technology* **2021**, *63*, 102531, https://doi.org/10.1016/j.jddst.2021.102531.
16. Beagan, A.M.; Alghamdi, A.A.; Lahmadi, S.S.; Halwani, M.A.; Almeataq, M.S.; Alhazaa, A.N.; Alotaibi, K.M.; Alswieleh, A.M. Folic acid-terminated poly (2-diethyl amino ethyl methacrylate) brush-gated magnetic mesoporous nanoparticles as a smart drug delivery system. *Polymers* **2021**, *13*, 59, https://doi.org/10.3390/polym13010059.

17. Karimi, B.; Emadi, S.; Safari, A.A.; Kermanian, M. Immobilization, stability and enzymatic activity of albumin and trypsin adsorbed onto nanostructured mesoporous SBA-15 with compatible pore sizes. *RSC Advances* **2014**, *4*, 4387-4394, http://doi.org/10.1039/c3ra46002a.
18. Pohaku Mitchell, K.K.; Liberman, A.; Kummel, A.C.; Trogler, W.C. Iron (III)-doped, silica nanoshells: a biodegradable form of silica. *Journal of the American Chemical Society* **2012**, *134*, 13997-14003, http://doi.org/10.1021/ja3036114.
19. Shao, H.; Qi, J.; Lin, T.; Zhou, Y. Preparation and Characterization of Fe3O4@ SiO2@ NMDP core-shell structure composite magnetic nanoparticles. *Ceramics International* **2018**, *44*, 2255-2260, http://doi.org/10.1016/j.ceramint.2017.10.184.
20. Li, G.; Shen, B.; He, N.; Ma, C.; Elingarami, S.; Li, Z. Synthesis and characterization of Fe3O4@ SiO2 core–shell magnetic microspheres for extraction of genomic DNA from human whole blood. *Journal of nanoscience and nanotechnology* **2011**, *11*, 10295-10301, https://doi.org/10.1166/jnn.2011.5200.
21. Sun, L.; Hong, X.; Zou, P.; Chu, X.; Liu, Y. Preparation and characterization of multifunctional Fe3O4/ZnO/SiO2 nanocomposites. *Journal of alloys and compounds* **2012**, *535*, 91-94, http://doi.org/10.1016/j.jallcom.2012.04.103.
22. Rashidzadeh, H.; Salimi, M.; Sadighian, S.; Rostamizadeh, K.; Ramazani, A. In vivo antiplasmodial activity of curcumin-loaded nanostructured lipid carriers. *Current drug delivery* **2019**, *16*, 923-930, http://doi.org/10.2174/1567201816666191029121036.
23. Hariani, P.L.; Faizal, M.; Ridwan, R.; Marsi, M.; Setiabudidaya, D. Synthesis and properties of Fe3O4 nanoparticles by coprecipitation method to removal procion dye. *International Journal of Environmental Science and Development* **2013**, *4*, 336-340, http://doi.org/10.7763/IJESD.2013.V4.366.
24. Tang, S.; Zhao, M.; Yuan, D.; Li, X.; Wang, Z.; Zhang, X.; Jiao, T.; Ke, J. Fe3O4 nanoparticles three-dimensional electro-peroxydisulfate for improving tetracycline degradation. *Chemosphere* **2021**, *268*, 129315, https://doi.org/10.1016/j.chemosphere.2020.129315.
25. Stöber, W.; Fink, A.; Bohn, E. Controlled growth of monodisperse silica spheres in the micron size range. *Journal of colloid and interface science* **1968**, *26*, 62-69, https://doi.org/10.1016/0021-9797(68)90272-5.
26. Wang, J.; Yang, J.; Li, X.; Wei, B.; Wang, D.; Song, H.; Zhai, H.; Li, X. Synthesis of Fe3O4@ SiO2@ ZnO–Ag core–shell microspheres for the repeated photocatalytic degradation of rhodamine B under UV irradiation. *Journal of Molecular Catalysis A: Chemical* **2015**, *406*, 97-105, https://doi.org/10.1016/j.molcata.2015.05.023.
27. Lv, X.; Huang, W.; Ding, X.; He, J.; Huang, Q.; Tan, J.; Cheng, H.; Feng, J.; Li, L. Preparation and photocatalytic activity of Fe3O4@ SiO2@ ZnO:La. *Journal of Rare Earths* **2020**, *38*, 1288-1296, https://doi.org/10.1016/j.jre.2020.04.007.
28. Khalkhali, M.; Sadighian, S.; Rostamizadeh, K.; Khoeini, F.; Naghibi, M.; Bayat, N.; Habibizadeh, M.; Hamidi, M. Synthesis and characterization of dextran coated magnetite nanoparticles for diagnostics and therapy. *BioImpacts: BI* **2015**, *5*, 141, https://doi.org/10.15171/bi.2015.19.
29. Sundrarajan, M.; Ramalakshmi, M. Novel cubic magnetite nanoparticle synthesis using room temperature ionic liquid. *E-Journal of Chemistry* **2012**, *9*, 1070-1076, https://doi.org/10.1155/2012/541254.
30. Handore, K.; Bhavsar, S.; Horne, A.; Chhattise, P.; Mohite, K.; Ambekar, J.; Pande, N.; Chabukswar, V. Novel green route of synthesis of ZnO nanoparticles by using natural biodegradable polymer and its application as a catalyst for oxidation of aldehydes. *Journal of Macromolecular Science, Part A* **2014**, *51*, 941-947, https://doi.org/10.1080/10601325.2014.967078.
31. Kotcherlakota, R.; Barui, A.K.; Prashar, S.; Fajardo, M.; Briones, D.; Rodríguez-Diéguez, A.; Patra, C.R.; Gómez-Ruiz, S. Curcumin loaded mesoporous silica: an effective drug delivery system for cancer treatment. *Biomaterials science* **2016**, *4*, 448-459, https://doi.org/10.1039/c5bm00552c.
32. Zak, A.K.; Razali, R.; Abd Majid, W.H.; Darroudi, M. Synthesis and characterization of a narrow size distribution of zinc oxide nanoparticles. *International journal of nanomedicine* **2011**, *6*, 1399, https://doi.org/10.2147/IJN.S19693.
33. Ebrahimzadeh, M.A.; Mortazavi-Derazkola, S.; Zazouli, M.A. Eco-friendly green synthesis of novel magnetic Fe3O4/SiO2/ZnO-Pr6O11 nanocomposites for photocatalytic degradation of organic pollutant. *Journal of Rare Earths* **2020**, *38*, 13-20, https://doi.org/10.1016/j.jre.2019.07.004.
34. Hajizadeh, Z.; Valadi, K.; Taheri-Ledari, R.; Maleki, A. Convenient Cr (VI) removal from aqueous samples: executed by a promising clay-based catalytic system, magnetized by Fe_3O_4 nanoparticles and functionalized with humic acid. *Chemistry Select* **2020**, *5*, 2441-2448, https://doi.org/10.1002/slct.201904672.

35. Hasan, M.; Elkhoury, K.; Kahn, C.J.; Arab-Tehrany, E.; Linder, M. Preparation, characterization, and release kinetics of chitosan-coated nanoliposomes encapsulating curcumin in simulated environments. *Molecules* **2019**, *24*, 2023, http://doi.org/10.3390/molecules24102023.